



# A plant-insertable multi-enzyme biosensor for the real-time monitoring of stomatal sucrose uptake

Shiqi Wu<sup>a</sup>, Wakutaka Nakagawa<sup>a</sup>, Yuki Mori<sup>b</sup>, Saman Azhari<sup>a</sup>, Gábor Méhes<sup>a</sup>,  
Yuta Nishina<sup>c,d</sup>, Tomonori Kawano<sup>b</sup>, Takeo Miyake<sup>a,\*</sup>

<sup>a</sup> Graduate School of Information, Production and Systems, Waseda University, Kitakyushu, 808-0135, Japan

<sup>b</sup> Faculty and Graduate School of Environmental Engineering, The University of Kitakyushu, Kitakyushu, 808-0135, Japan

<sup>c</sup> Research Institute for Interdisciplinary Science, Okayama University, Okayama, 700-8530, Japan

<sup>d</sup> Institute for Aqua Regeneration, Shinshu University, 390-8621, Matsumoto, Japan

## ARTICLE INFO

### Keywords:

Flexible wearable sensor  
Plant monitoring  
Carbon fiber  
Multi-enzyme system

## ABSTRACT

Monitoring sucrose transport in plants is essential for understanding plant physiology and improving agricultural practices, yet effective sensors for continuous and real-time in-vivo monitoring are lacking. In this study, we developed a plant-insertable sucrose sensor capable of real-time sucrose concentration monitoring and demonstrated its application as a useful tool for plant research by monitoring the sugar-translocating path from leaves to the lower portion of plants through the stem in living plants. The biosensor consists of a bilirubin oxidase-based biocathode and a needle-type bioanode integrating glucose oxidase, invertase, and mutarotase, with the two electrodes separated by an agarose gel for ionic connection. The sensor exhibits a sensitivity of  $6.22 \mu\text{A mM}^{-1} \text{cm}^{-2}$ , a limit of detection of  $100 \mu\text{M}$ , a detection range up to  $60 \text{mM}$ , and a response time of  $90 \text{s}$  at  $100 \mu\text{M}$  sucrose. Additionally, the sensor retained  $86 \%$  of its initial signal after  $72 \text{h}$  of continuous measurement. Day-night monitoring from the biosensor inserted in strawberry guava (*Psidium cattleianum*) showed higher sucrose transport activity at night, following well the redistribution of photosynthetically produced sugars. In addition, by monitoring the forced translocation of sucrose dissolved in the stable isotopically labeled water, we demonstrated that a young seedling of Japanese cedar known as Sugi (*Cryptomeria japonica*) can absorb and transport both water and sucrose through light-dependently opened stomata, which is the recently revealed path for liquid uptake by higher plants. These findings highlight the potential of our sensor for studying dynamic plant processes and its applicability in real-time monitoring of sugar transport under diverse environmental conditions.

## 1. Introduction

Enzymatic biosensors have been widely used and developed for various applications, such as medical diagnoses (Huang et al., 2017; Ispas et al., 2012), environmental monitoring (Justino et al., 2017; Purcarea et al., 2024), food and beverage industry (Gavrilaş et al., 2022; Shankaran et al., 2007), and biotechnology and pharmaceuticals (Wang et al., 2023; Yan et al., 2011; Zhou et al., 2023). Thanks to the specific catalytic character of enzymes, these biosensors could detect and quantify various targeted analytes. At the current state, the research of enzymatic biosensors is mainly focusing on human health applications, including disease detection and diagnosis (Hemdan et al., 2024; Tang and Ren, 2008), therapeutic drug monitoring (Alvau et al., 2018; Kai et al., 2017; Ogawa et al., 2015), wearable health monitoring devices (Li

et al., 2023; Song et al., 2023; Ye et al., 2020), and point-of-care testing (Bihar et al., 2016; Kulkarni et al., 2022; Lu et al., 2023). Enzymatic biosensors for glucose have also been used to monitor blood sugar levels in animals (Bruen et al., 2017; Makaram et al., 2014; Miyake et al., 2011a).

Despite the wide use of enzymatic biosensors in humans, animals, and insects, the applications in plants are relatively few, particularly for monitoring plant metabolites (Perdomo et al., 2023; Taniguchi et al., 2020). There are some publications on real-time glucose monitoring from sap, root exudates, and even chloroplasts (Table S1). However, other than glucose, one of the important and common plant metabolites is sucrose, which plays a crucial role in plant physiology as a primary product of photosynthesis and a major transport sugar (Huber and Huber, 1992; Lastdrager et al., 2014; Sturm, 1999). In most higher

\* Corresponding author.

E-mail address: [miyake@waseda.jp](mailto:miyake@waseda.jp) (T. Miyake).

<https://doi.org/10.1016/j.bios.2025.117674>

Received 11 March 2025; Received in revised form 31 May 2025; Accepted 6 June 2025

Available online 8 June 2025

0956-5663/© 2025 The Authors. Published by Elsevier B.V. This is an open access article under the CC BY-NC-ND license (<http://creativecommons.org/licenses/by-nc-nd/4.0/>).

plants, glucose produced via photosynthesis is rapidly converted into sucrose in the cytosol before being loaded into the phloem. Sucrose then acts as the main form of long-distance carbon transport, moving from source tissues such as mature leaves to sink tissues like roots, young leaves, and developing fruits (Lemoine et al., 2013; Ruan, 2014). Once delivered, sucrose is metabolized by enzymes including invertase and sucrose synthase, which support its further utilization in energy production and biosynthetic pathways such as starch and cellulose synthesis. Real-time monitoring of sucrose concentrations within plants could provide valuable data on plant health, growth, and response to environmental conditions. Nevertheless, the development of enzymatic sensors for real-time sucrose monitoring in plants faces several challenges, including the complex and variable plant shape, the need for miniaturization and integration of sensors into plant tissues without causing damage, and ensuring the sensors' sensitivity and selectivity in the plant's environment. In response to these challenges, researchers are exploring more refined monitoring technologies to reveal the complex responses of plants to environmental changes.

One such environmental change involves water exchange process and the uptake of nutrients dissolved in water (Cao et al., 2015; Trommelen et al., 2017). Water physiology is very important in higher plants, but there are still many unclear points regarding the fates of water in vivo and the mechanism of water exchange between the aerial parts of plants and the surrounding environments. Conventionally, a model has been used in which the root system is solely involved in the uptake of the liquid form of water and the discharge of water through transpiration by which the gaseous form of water (vapor) is released in the air through the stomatal opening on the leaves. Therefore, it is well considered that regulation of stomatal opening plays a central role in plant water physiology in living plants. However, numerous recent observations suggest that plants may also absorb water through alternative pathways. Many lower plants can readily absorb water through their surfaces (Berry et al., 2019; Chin et al., 2023; Dawson and Goldsmith, 2018). In arid environments, the desert plant, *Syntrichia caninervis*, has been observed to capture water from fog (Berry et al., 2019; Pan et al., 2016). Even in higher plants, certain phenomena indicate that the cuticle may play a role in water absorption (Boaneres et al., 2018; Guzmán-Delgado et al., 2021). For example, fruit growers have often noted that cherries and other fruits crack after maturing, especially when exposed to prolonged rain, due to excess water on the fruit surface (Knoche, 2015; Louise Hovland \* and Sekse, 2004). Moreover, studies have demonstrated that blue light induces stomata opening, thereby allowing water uptake into the plant's water cycle. Our preliminary demonstrations with model plants, such as the hydroponically grown seedlings of lettuce, revealed that stomata opening in response to light can serve as a pathway for the uptake of liquid water, in addition to the outward movement of vapor (Noda et al., 2025). These findings promoted us to verify a new water physiological model in which stomata contributes to water exchange. In this preliminary study, we used young seedlings of Japanese cedar known as Sugi (*Cryptomeria japonica*) as a model to confirm the movement of liquid water and solute (sucrose) through light-regulated stomata.

However, verifying such a physiological model requires tools capable of monitoring solute transport—in particular, sucrose—continuously, quantitatively, and in real time within intact plant tissues. This demand highlights the need for biosensing technologies that can operate stably inside living plants, detect low concentrations of sucrose, and withstand mechanical and environmental challenges. To date, enzymatic biosensors for plant sucrose monitoring have made substantial progress in form factor and integration. For example, Diacci et al. (2021) developed an organic electrochemical transistor (OECT)-based sensor capable of continuous monitoring for up to 48 h. However, this platform only enabled qualitative tracking of sucrose levels in plants and was not suitable for quantitative analysis. In addition, its patch-like structure limits its applicability in mechanically rigid plant tissues and may suffer from low resistance to physical disturbances. More recently

(Chen et al., 2024), introduced a microneedle-based enzymatic sensor that enabled real-time glucose monitoring in plant stems. With a reported sensitivity of  $17 \text{ nA } \mu\text{M}^{-1} \text{ cm}^{-2}$ , the sensor was demonstrated on soft-tissue plants such as aloe and tomato. However, due to the fixed length and depth of the microneedle array, its applicability to woody or structurally rigid plant tissues remains limited, and the inability to adjust the insertion depth restricts its use across diverse plant species with varying sap flow depths.

To overcome these limitations and enable real-time monitoring of dynamic sucrose changes within plant tissues—particularly those introduced via light-regulated stomatal water uptake—we developed a needle-type implantable enzymatic biosensor capable of minimally invasive integration into a wide range of plant structures (Fig. 1), achieving sensitivity of  $6.22 \text{ } \mu\text{A mM}^{-1} \text{ cm}^{-2}$ ,  $100 \text{ } \mu\text{M}$  limit of detection (LOD), and operational stability beyond 72 h of continuous measurement. The anode uses a multienzyme electrode with a mixture of glucose oxidase (GOD) and mutarotase (MUT) covered with invertase (INV), while the cathode uses bilirubin oxidase (BOD), the latter reported previously (Yin et al., 2019, 2020, 2021). Our biosensor can provide continuous measurements of sucrose levels with a low LOD and wide detection range. To achieve this, the insertion device is designed so that the oxidation current from sucrose at the anode is lower than the reduction current from oxygen at the cathode to extend the operation lifetime. Furthermore, the use of carbon fibers as base electrodes ensures a compact, disposable, and environmentally friendly sensor with a form factor highly integrable with plants. Thus, our sensor has considerable potential applications in agriculture and horticulture. Moreover, we applied the sensor for real-time monitoring of sucrose uptake through cedar leaf stomata during light and dark exposure cycles. Using this implantable sucrose sensor, we can observe the immediate response of plants to light, wherein sucrose uptake through the stomata is significantly enhanced during light exposure compared to dark periods. This real-time monitoring device provides a method for precision agriculture, allowing for the optimization of growth conditions and a better understanding of plant responses to environmental changes.

## 2. Materials and methods

### 2.1. Materials

Carbon fibers were obtained from FC-R&D Corp. (Sagamihara, Japan). TUBALL SWCNT solution (01RW03) was obtained from Kusumoto Chemicals, Ltd. (Tokyo, Japan). Polyvinylimidazole-[Os(bipyridine)<sub>2</sub>Cl] (PVI-Os) was donated by Research Core for Interdisciplinary Sciences, Okayama University. Glucose oxidase (GOD, solid, from *Aspergillus* sp., 180 U/mg) and Invertase (INV, solid, from *Candida* sp., 100 U/mg) were purchased from TOYOBO Biotechnology operating department (Osaka, Japan). Mutarotase (MUT, suspension, from porcine kidney, 10000 U/mL), monopotassium phosphate, and dipotassium phosphate were purchased from FUJIFILM Wako Pure Chemical Corporation (Osaka, Japan). Bilirubin oxidase (BOD, solid, from *Myrothecium* sp., 10 U/mg) was purchased from Amano Enzyme Inc. (Nagoya, Japan). Glutaraldehyde (Grade II, 25 % in H<sub>2</sub>O) was purchased from Sigma Aldrich. Charge pump IC (S-882Z20, input voltage (0.3–3 V), output voltage (VIC, 2V), discharge starting voltage: 2.4 V, and shutdown voltage: 2.5 V) was purchased from Mouser Electronics, Inc. (Texas, USA). Deionized water made by Kitakyushu tap water was used as a source of fresh water for plants. For water tracing experiments, Kitakyushu tap water and commercially available bottled Alaskan glacial water (Alaskan Glacier Products Chugiak, Alaska, USA) sampled from Eklutna Lake, Alaska state, USA, was used.

### 2.2. Preparation of sucrose bioanode

The preparation of bioanode and related materials' characterizations was based on our previous work (Yin et al., 2019, 2020, 2021). In short,

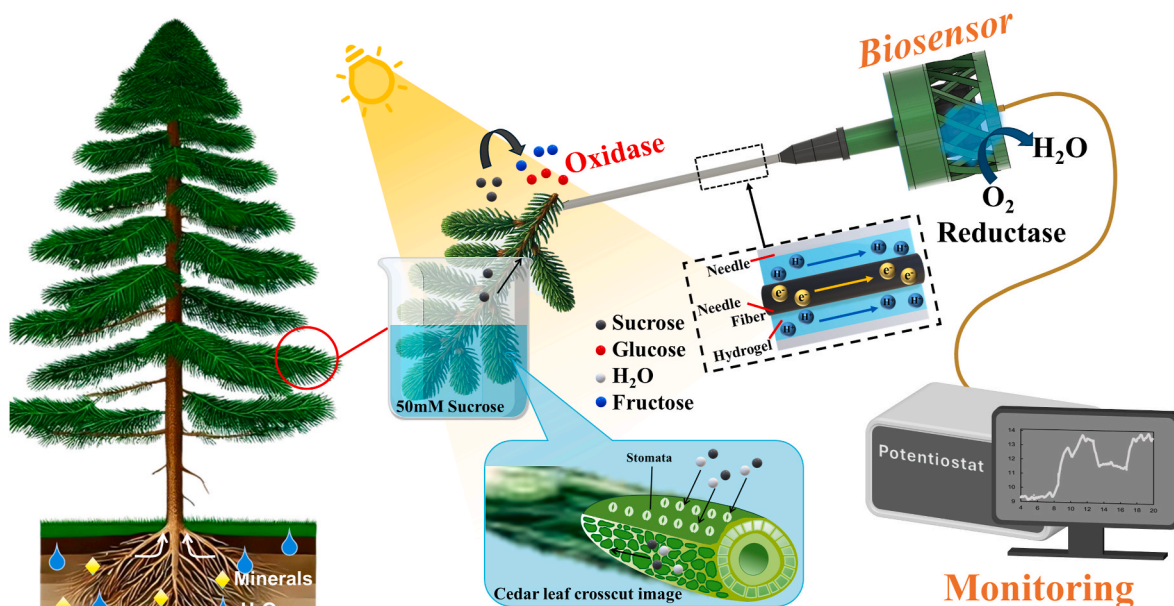


Fig. 1. Schematic figure of the needle-type implantable enzymatic biosensor specifically designed for real-time monitoring of sucrose concentrations within plant tissues.

5 cm long carbon fiber (CF) was dip-coated in a 50  $\mu\text{L}$  SWCNT solution (TUBALL), then dried at 90  $^{\circ}\text{C}$  on a hot plate for 10 min, repeated thrice. The coated SWCNT/CF was then washed in distilled water for 30 min to remove loosely attached SWCNT. For further functionalization, the SWCNT/CF was immersed into a PVI-Os solution while stirring at 4  $^{\circ}\text{C}$  for 2 h, followed by 30 min of washing in distilled water. The GOD-MUT solution was made by mixing GOD (1.5 mg/mL), MUT (12.5  $\mu\text{L}/\text{mL}$ ), glutaraldehyde (12.5  $\mu\text{L}/\text{mL}$ ), and phosphate-buffered saline (PBS, 50 mM  $\text{KH}_2\text{PO}_4$ , pH = 7) solutions. The INV solution was made by mixing INV (2.5 mg/mL), glutaraldehyde (12.5  $\mu\text{L}/\text{mL}$ ), and PBS (50 mM). Then, the PVI-Os/SWCNT/CF was immersed into a GOD-MUT solution under stirring at 4  $^{\circ}\text{C}$  for 2 h, followed by immersing the (GOD-MUT)/PVI-Os/SWCNT/CF in INV solution under stirring at 4  $^{\circ}\text{C}$  for 2 h.

### 2.3. Preparation of $\text{O}_2$ -Diffusion bilirubin biocathode

The  $\text{O}_2$ -diffusion biocathode was fabricated and optimized using the method reported in our previous work (Yin et al., 2019, 2020, 2021). The CF fabric was cut into a 15 mm  $\times$  15 mm square shape. Then, the CF fabric was dip-coated with a 225  $\mu\text{L}$  SWCNT solution (TUBALL) and then dried at 90  $^{\circ}\text{C}$  on a hot plate for 10 min. This process was repeated thrice. The coated SWCNT/CF was then washed in distilled water for 30 min to remove loosely attached SWCNT. This step will also remove the surfactant contained in the product and make CNT hydrophobic. Then, the SWCNT/CF was cut into a ring shape with an outer diameter of 12 mm and an inner diameter of 4 mm. The SWCNT/CF was then immersed into a solution of bilirubin oxidase (5 mg/mL) in 50 mM PBS solution, under stirring at 4  $^{\circ}\text{C}$  for 12 h.

### 2.4. Electrochemical measurements and biosensor assembly and testing (non-needle form)

The electrochemical properties of the enzymatic sucrose sensor were systematically evaluated to assess its responsiveness, stability, and suitability for real-time monitoring. Chronoamperometry and cyclic voltammetry (CV) were employed to quantify current responses and characterize the sensor's behavior under varying sucrose concentrations and environmental conditions. For bioanode and biocathode testing, both electrodes were connected as the working electrode, while a platinum wire electrode was used as the counter electrode, and a wire Ag/

AgCl (3 M KCl) electrode served as the reference electrode. To evaluate the responsivity of the sucrose sensor, the experimental setup involved stirring 8 mL of 22  $^{\circ}\text{C}$  PBS solution while incrementally adding high-concentration sucrose solutions (0.5 M) in volumes of 1.6  $\mu\text{L}$  (equivalent to 0.1 mM) and 16  $\mu\text{L}$  (equivalent to 1 mM). The full sensor was tested in 5 mL PBS while stirring.

### 2.5. Preparation and testing of needle-type injection device

The needle-type injection device is composed of an injection needle (18G, Terumo), a custom-made 3D-printed (Form 3+, Formlabs, USA) needle holder, and enzymatic bioelectrodes (Fig. S1). To expose the enzyme electrodes and increase the surface area available for chemical reactions, the tip of the needle was modified by creating holes (0.8 mm diameter) with a grinder, as mentioned in previous work (Yin et al., 2020). The sucrose sensing bioanode length exposed at the needle tip was standardized at 15 mm to ensure consistent performance across various samples and to maintain the structural integrity of the needle. The agarose solution (1 wt %) was filled and solidified inside the needle and the needle holder, allowing the protons to move through the agarose gel between bioanode and biocathode. Oxygen diffusion through the holes in the needle holder happens via the agarose gel to the biocathode as well.

### 2.6. Evaluation of water uptake by tracing the stable isotope ratio

To investigate plant metabolic pathways, traditional methods such as fluorescence labeling, isotope labeling, and radioactive tracers have been widely used. However, fluorescence labeling is often limited by the natural pigmentation of plant leaves, which can interfere with fluorescence signals and reduce the accuracy of the results. Similarly, radioactive tracers, while highly sensitive, pose safety concerns and are less practical for experiments involving living plants over extended periods. To overcome these challenges, we employed isotope labeling as an alternative. Isotope labeling is non-invasive, safe, and capable of providing precise insights into metabolic pathways. Specifically, we utilized water from two different regions with distinct oxygen-18 ( $^{18}\text{O}$ ) isotope compositions. It is well-established that water from different geographical sources contains varying  $^{18}\text{O}$  isotope levels due to environmental and climatic factors. By using these naturally varying  $^{18}\text{O}$

compositions, we could track water uptake through leaf stomata and determine whether plants absorb water directly from their leaf surfaces. This approach not only avoids the limitations of other methods but also leverages natural isotopic variations to study plant water absorption processes effectively.

Physicochemical analysis of water intake by typical coniferous leaf tissues of intact living Sugi seedlings was performed according to the protocol proposed by Kawano Lab (Noda et al., 2025). Briefly, the detection and quantification of stable isotopes of oxygen ( $^{18}\text{O}$  over oxygen-16 ( $^{16}\text{O}$ )) in the water samples or leaf extracts (1  $\mu\text{L}$ , each) loaded to Ag capsules were carried out by using a stable isotope ratio mass spectrometer (IsoPrime100; IsoPrime, Cheadle, UK) connected with an element (CNSOH) analyzer (vario PYRO cube; IsoPrime, Cheadle, UK).

### 3. Results and discussion

#### 3.1. Description of the sensing concept

Biofuel cell (BFC)-type devices are traditionally employed for power generation due to their ability to efficiently convert chemical energy into electrical energy. However, as shown in Fig. 1, in this study, we adapted a BFC for sucrose sensing, leveraging this technology to achieve real-time and highly sensitive detection. The enzymatic bioanode and biocathode were designed to maximize the precision of substrate detection, ensuring that the device output directly corresponds to the measured sucrose concentration rather than to energy generation. This design offers several advantages over conventional sensing devices. First, the integration of a multi-enzyme bioanode (glucose oxidase, mutarotase, and invertase) enables efficient and sequential catalysis of sucrose, producing electron transfer directly proportional to sucrose concentration. Second, the oxygen diffusion biocathode, based on bilirubin oxidase, facilitates stable reduction reactions under air-saturated conditions. Additionally, the use of PVI-Os as an embedded electron transfer mediator in the bioanode significantly enhances electron transfer efficiency compared to traditional systems that rely on freely diffusing mediators. Together, these features should ensure high sensitivity, rapid response times, and a wide detection range.

Specifically, the multi-enzyme bioanode acted on sucrose by catalyzing it into gluconic acid in three steps. First, invertase catalyzed the breakdown of sucrose into  $\alpha$ -glucose and fructose. Then, mutarotase converted  $\alpha$ -glucose into  $\beta$ -glucose. Finally, glucose oxidase catalyzed the oxidation of  $\beta$ -glucose into gluconic acid at the anode.  $\alpha$ -glucose and  $\beta$ -glucose are two isomeric forms of glucose, differing in the orientation of the hydroxyl group (Chiba, 1997; Hudson, 1910). Both forms exist naturally, with an approximate ratio of  $\alpha$ -glucose to  $\beta$ -glucose of 9:16 (Weng et al., 2023). Since glucose oxidase can only catalyze the oxidation of  $\beta$ -glucose (Mano, 2019), the use of mutarotase to convert  $\alpha$ -glucose is essential.

Our device also incorporates an agarose gel interface to prevent short-circuiting while enabling efficient proton transfer between the bioanode and biocathode. These modifications make the sensor highly adaptable to varying environmental conditions, such as temperature and oxygen availability, and improve its reliability for *in vivo* plant monitoring. The choice of carbon material ensures that the electrodes do not pollute the environment and do not negatively impact the commercial or edible value of plants. By adapting a fuel cell-type technology for sensing applications, this sensor bridges the gap between energy devices and biosensing applications, offering a robust platform for studying dynamic plant processes with high precision and efficiency.

#### 3.2. Electrochemical performance of bioanode, biocathode, and the complete enzymatic sensing system

The ratio of INV: MUT: GOD is 2:1:2. A previous study by Hamid J.A. et al. (Hamid et al., 1988) reported an effective ratio of 10:5:1 for a

similar multi-enzyme system, but in a different electrode material. In our multi-enzyme system, GOD is the only enzyme responsible for transferring electrons to the electrode mediated by PVI-Os. To ensure that the glucose generated by INV and MUT could be fully utilized by GOD, we increased the amount of GOD and set its concentration equal to that of INV. The revised ratio was evaluated using cyclic voltammetry in Fig. S2. The results showed that the oxidation peak was significantly higher with the 2 : 1 : 2 ratio compared to the 10 : 5 : 1 ratio for our electrode, confirming that the new combination improved the overall signal output. Therefore, this ratio was used for all subsequent experiments.

For the multi-enzyme system (Fig. 2a(i)), it is important to properly arrange the immobilization sequence of the three enzymes to align with the reaction steps. As shown in Fig. 2a(ii), based on spatial structure simulation of INV, MUT, and GOD, INV appears as an ellipsoid, MUT as a cylinder, and GOD has a flattened disk shape (Alberto et al., 2004; Thoden and Holden, 2002; Wohlfahrt et al., 1999). Despite the differences in shape, the sizes of these enzymes are similar, allowing us to try various sequences of immobilizations without worrying that larger enzymes would block smaller ones. Therefore, we tested the following enzyme immobilization sequences: 1) immersion in a GOD and MUT mixed solution followed by an INV solution ((GOD + MUT), INV); 2) immersion in a mixed solution of GOD, MUT, and INV all together (GOD + MUT + INV); 3) immersion first in a GOD solution, followed by a mixture of MUT and INV (GOD, (MUT + INV)); and 4) immersion in each of GOD, MUT, and INV solutions in this order (GOD, MUT, INV).

Chronoamperometry was employed to measure the current outputs of bioanodes with four different enzyme immobilization sequences in stirred PBS solutions containing sucrose at concentrations from 0.1 to 100 mM in increments of two- or five-fold. Fig. 2b shows that after having tried sequences 1–4, sequence 1, *i.e.*, immersing the electrode first in a GOD and MUT mixed solution, followed by an INV solution (red dots), resulted in the highest current density (12.08  $\mu\text{A}/\text{cm}^2$  at 50 mM sucrose). We hypothesize that this sequence allows GOD and MUT to be immobilized in the inner layer closer to the electrode material, facilitating electron transfer and enabling the newly formed  $\beta$ -glucose to be immediately oxidized by the adjacent GOD. Meanwhile, subsequent immobilization of INV on the electrode surface maximized the contact area with sucrose, thereby enhancing the conversion of sucrose to  $\alpha$ -glucose. Moreover, the LOD was determined based on the standard deviation of the blank signal and the logarithmic calibration curve. Using the criterion of  $S/N = 3$ , the LOD was calculated to be 100  $\mu\text{M}$ , corresponding to a current response of 1.175  $\mu\text{A}$ .

At a sucrose concentration of 100 mM, the current level of (GOD + MUT), INV was nearly identical to that of (GOD + MUT + INV), suggesting the catalytic limit of the electrode was reached. However, at a sucrose concentration of 50 mM, the current level of the (GOD + MUT), INV configuration was significantly higher than that of the other groups. Therefore, we focused further experiments on ((GOD + MUT), INV) anode in different sucrose concentrations. As shown in the CV graph (Fig. 2c), the oxidation peak current increased linearly with sucrose concentration in the range from 0 mM to 60 mM, but there was only a little difference between the oxidation peak currents at 60 mM and 70 mM, indicating that the electrode had reached its catalytic limit at these concentrations.

Since the sucrose sensor developed in this study is a plant-insertable device, it should reliably operate under varying temperature conditions for real-world applications. These conditions may include day-night temperature fluctuations or controlled environments such as greenhouses. To understand the relationship between temperature and the sensor's electrical output, we evaluated its performance at different temperatures. In this experiment, a 10 mM sucrose PBS solution was initially cooled in a refrigerator and then stirred on a hot plate. CV measurements were performed when the solution reached specific temperatures of 10  $^{\circ}\text{C}$ , 22  $^{\circ}\text{C}$ , 30  $^{\circ}\text{C}$ , and 40  $^{\circ}\text{C}$ . The results, as shown in Fig. 2d, demonstrate that the sensor generates stable electrical signals

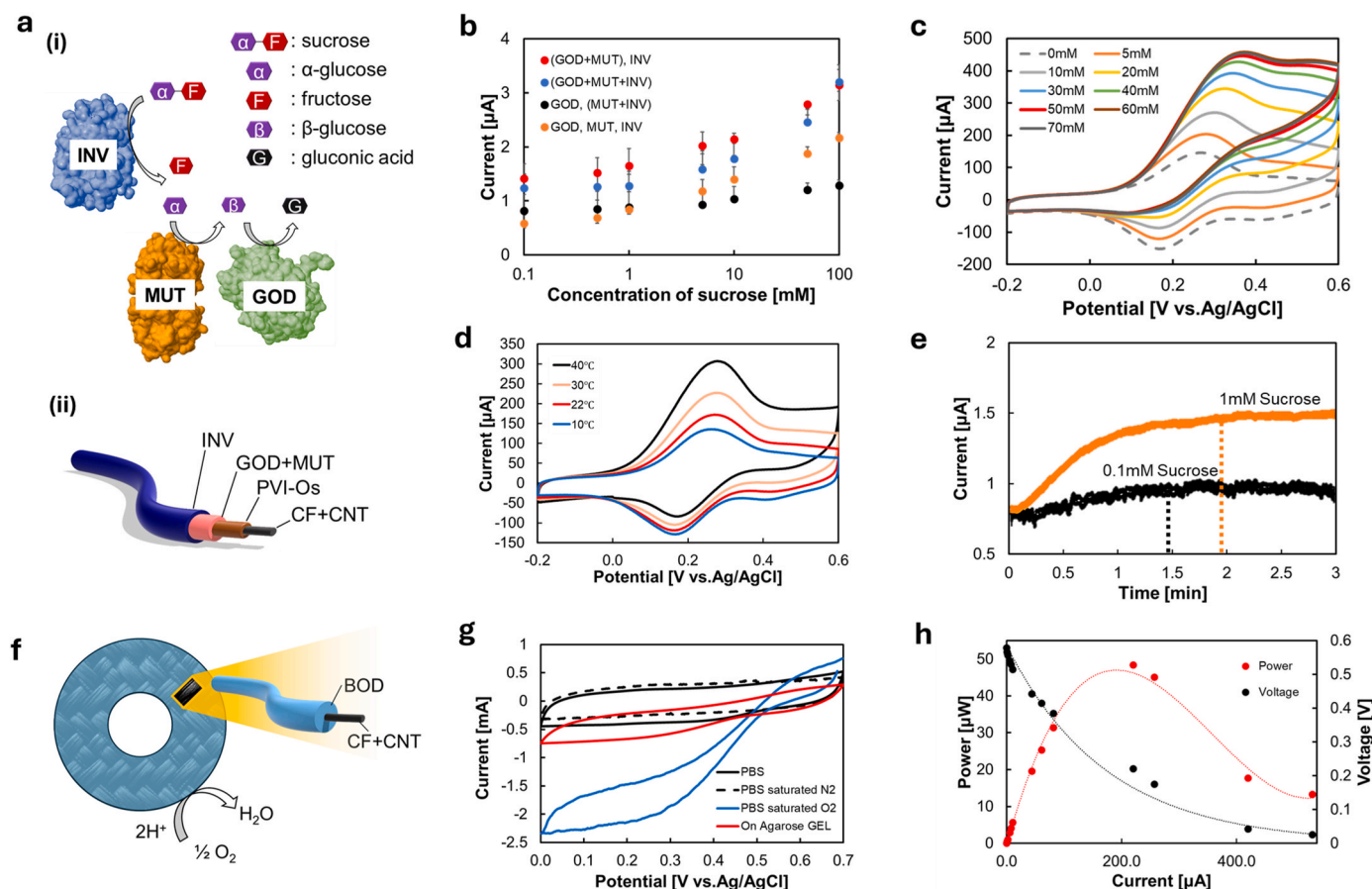


**Fig. 2. Electrochemical characterization of bioanode and biocathode.** a) Graphical illustrations of (i) the multi-enzyme system used in the bioanode for sucrose sensing and (ii) the spatial structure of bioanode. b) Concentration dependence of sucrose conversion by bioanode with different enzyme immobilization sequences in the range of sucrose concentrations from 0.1 to 100 mM, determined by chronoamperometric measurements at +0.6 V. CV scans of (GOD + MUT), INV bioanode at 10 mV·s<sup>-1</sup> in PBS (each point is the average and the error bars are the standard deviation between three samples (n = 3)) c) at different sucrose concentrations at 22 °C, and d) in 10 mM sucrose at 10 °C, 22 °C, 30 °C, 40 °C. e) Current response of (GOD + MUT), INV bioanode in 0.1 mM and 1 mM sucrose solutions, respectively. f) Schematic of the gas-diffusion BOD cathode used in the sensor. g) CV scans of biocathode at 10 mV s<sup>-1</sup> in PBS, PBS saturated with N<sub>2</sub>, PBS saturated with O<sub>2</sub> and on PBS absorbed agarose gel, at 22 °C. h) Power and polarization curves of the full biosensor in 50 mM sucrose.

across this temperature range. Furthermore, the signal intensity increased with rising temperature, indicating that moderately high temperatures enhance the electrochemical response of the sensor. These findings suggest that the sensor's performance is temperature-dependent, and the observed variations in signal intensity can be effectively standardized based on the measurement temperature. This temperature normalization allows for more accurate sucrose concentration readings in practical applications, ensuring reliable measurements across diverse environmental conditions.

To achieve real-time monitoring of sucrose concentrations, the immediate response of the sensor electrode to target sucrose molecules is critical. Thus, we measured the current generated by enzymatic reactions using chronoamperometry at a constant potential of +0.6 V vs Ag/AgCl (3 M KCl). As shown in Fig. 2e, the response time of the fabricated sucrose sensor was ~90 s and ~2 min for the addition of 0.1 mM and 1.0 mM sucrose, respectively. Compared to other sucrose sensors relying on hydrogen peroxide-mediated electron transfer, which typically requires around 5 min at the concentration of 5.6 mM (Scheller and Renneberg, 1983) for response, the highly efficient electron transfer of PVI-Os enabled faster electrode responses of 1.5 (0.1 mM) and 2 (1.0 mM) minutes, respectively. This rather fast response shows the potential of the sensor for practical real-time measurements, owing to the use of PVI-Os that significantly improve the efficiency of electron transfer, reducing the time required for the sensor to detect changes in sucrose concentration. Moreover, the sensitivity was calculated as total current

sensitivity ( $0.56 \mu\text{A mM}^{-1}$ ) divided by the electrode surface area ( $0.09 \text{ cm}^2$ ), yielding a current density sensitivity of  $6.22 \mu\text{A mM}^{-1} \text{ cm}^{-2}$ .

Next, to assess the efficiency of our gas-diffusion BOD cathode (Fig. 2f), we determined the reduction currents produced from atmospheric oxygen. During these measurements, the cathode was positioned on an agarose gel that had been saturated with PBS, and the other face of the cathode was exposed to air. Because of the low solubility and slow diffusion rate of dissolved oxygen in aqueous solutions, the BOD cathode relies heavily on an effective gas-diffusion electrode for highly catalytic performance. Due to the intrinsic structural properties of the SWCNT, the material exhibited high hydrophobicity, effectively promoting air oxygen contact with the electrode's surface.

As shown in Fig. 2g, the CV scans performed in PBS solution saturated by N<sub>2</sub> (dashed line) displayed no reduction current signal in the absence of oxygen. When the cathode was immersed into non-degassed PBS (black line), a distinct oxygen reduction peak was observed, attributable to the dissolved oxygen in the PBS. In contrast, when the electrode was placed on an agarose gel (red line), the surface of the cathode was exposed to air, resulting in a greater current compared to when it was fully submerged in PBS. This enhanced current is indicative of improved oxygen availability at the electrode surface. Finally, with PBS saturated with oxygen (blue line), the dissolved oxygen concentration reached saturation, resulting in a more pronounced enzymatic response by the BOD catalyst. This further confirmed that the reduction peak observed was associated with oxygen reduction, with the reduction

reaction initiating at approximately +0.55 V vs Ag/AgCl (3 M KCl).

Finally, the performance of the sucrose BFC-sensor, constructed from the functionalized multi-enzyme bioanode and oxygen diffusion biocathode is shown in Fig. 2h. In a 50 mM sucrose solution, an open circuit potential of 0.6 V was observed, which matches the value calculated as the sum of the anode (0.1 V, Fig. 2c) and cathode (0.5 V, Fig. 2g) reaction potentials. The maximum power of the sensor was measured to be 49  $\mu$ W at 0.21 V.

Moreover, to verify the temperature stability and reversibility of the device, we tested the sensor response to 50 mM sucrose solution under varying temperatures with the sequence of 10 °C  $\rightarrow$  22 °C  $\rightarrow$  30 °C  $\rightarrow$  40 °C  $\rightarrow$  30 °C  $\rightarrow$  22 °C  $\rightarrow$  10 °C (Fig. S3). The results demonstrate consistent signals at the same temperature, indicating that the sensor can maintain measurement accuracy despite temperature fluctuations.

### 3.3. Performance of the needle-type sensor in the fruit and stem of strawberry guava (*Psidium cattleianum*)

The cross-sectional view of the needle-shaped sucrose sensor developed in this study is illustrated in Fig. 3a. It consists of two main parts: the sensor body, which includes the agarose gel and electrodes, and the needle section, which partially encloses the bioanode. The sensor body is fabricated using 3D printing, with a mesh structure in the upper portion to allow free oxygen diffusion from the air to the biocathode. The biocathode, in the form of a disc, is positioned in the middle section, beneath which lies the agarose gel immersed into 50 mM PBS solution, serving as a medium for proton transport from the bioanode to the biocathode. A mesh-like tube surrounding the bioanode separates the two electrodes, preventing direct contact and a potential short-circuit while permitting free diffusion of liquid and protons.

The needle portion containing a commercially available standard hypodermic needle with a diameter of 1.2 mm allows for a smooth passage of the electrode and proper filling of the agarose gel within the needle. Additionally, as discussed in our previous work (Yin et al., 2020), the needle was modified to increase the bioanode's exposure to plant sap at the tip, thereby markedly shortening the response time of chemical measurements and facilitating the inflow of fresh sucrose-containing plant sap and the outflow of the used sap. This modification was realized by creating four openings in the needle tip

using a grinder, as shown in Fig. 3a. Since sucrose was transported in the phloem, which is located near the surface of stems and branches, precise insertion of the needle tip into this layer allows the biosensor to detect sucrose transported in the sap. The concentration of sucrose in this region is regulated by the plant itself and is not affected by the insertion process, as long as the correct tissue layer is reached.

To test our sensor, we measured the sucrose concentration in strawberry guava. Before performing this experiment, as a proof of concept first we wanted to see whether this BFC-type sensor can generate enough power to light up an LED. Therefore, as described in our previous work (Miyake et al., 2011a, 2011b), we combined the sucrose sensor with a blinking device that includes a charge pump integrated circuit (Fig. 3b(i)), a red light-emitting diode (LED), and a 0.47  $\mu$ F capacitor. Since the LED has a driving voltage of 1.7 V and the open-circuit potential of the sucrose sensor in this study is 0.6 V, we used a booster circuit to deliver enough voltage to the LED (Fig. 3b(i)). Upon insertion into the fruit of the strawberry guava, the sucrose sensor detects an electrical signal generated from the sucrose in the sap, which is then stored in the capacitor. When the capacitor accumulates sufficient charge, the charge pump circuit discharges, producing a 1.7 V voltage that momentarily lights the LED, creating a blink. A higher sucrose concentration results in a stronger electric signal that fills the 0.47  $\mu$ F capacitor in a shorter time, leading to a higher blinking frequency, which in turn reflects the sucrose concentration in the fruit of strawberry guava.

To calibrate the blinking frequency to sucrose concentration, we counted the number of blinks of the LED for PBS solutions with sucrose concentrations of 5, 10, 30, and 40 mM, as well as when inserted into strawberry guava, with measured frequencies of 0.46 Hz, 0.77 Hz, 3.34 Hz, 4.98 Hz, and 4.64 Hz, respectively (Fig. 3b(ii)). The last value (4.64 Hz) was measured in strawberry guava, corresponding to a sucrose concentration of  $\sim$ 38 mM.

Fig. 3c(i) shows the real-time sucrose concentration monitoring in plant sap in the stem of a strawberry guava plant grown in soil over 24 h. The sensor was operated in a chronoamperometric regime with a fixed potential of +0.6 V, and changes in the measured current correspond to changes in sucrose concentration, as shown in Fig. 3c(ii). Sucrose concentration decreased progressively to 2.22 mM during the daytime, while at night, it steadily increased to 4.3 mM, which concentration is

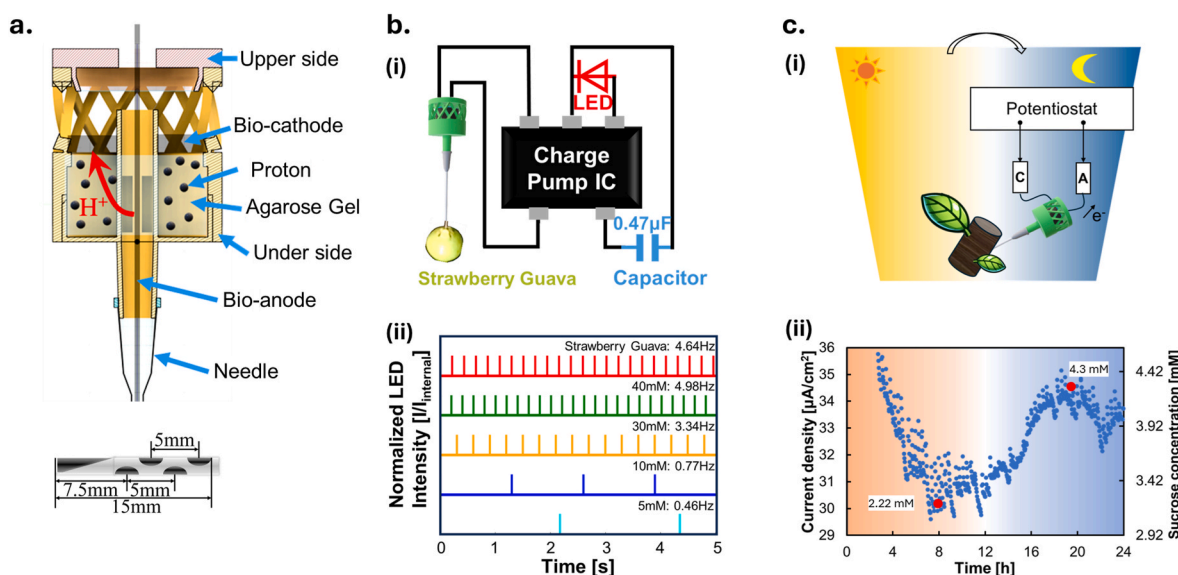


**Fig. 3.** a) Schematic for the cross-sectional view of the needle-shaped sucrose sensor. b) (i) Schematic of sucrose measurement circuit in the fruit of strawberry guava with blinking device that includes a charge pump integrated circuit; (ii) blink frequency of the LED measured in strawberry guava and in solutions of different sucrose concentrations (SI video1). c) (i) Schematic for real-time day-night monitoring of sucrose concentration in the stem of the strawberry guava plant using a potentiostat; (ii) 24-h monitoring of sucrose.

within the physiological range (Secchi and Zwieniecki, 2016). This pattern suggests that sucrose transport is more active at night. During the day, under sunlight exposure, the plant leaves produce glucose through photosynthesis, generating and accumulating sugars as nutrients. However, when photosynthesis ceases at night, the accumulated sugars are transported through the stem's vascular system to supply the entire plant. Studies have indicated that plants tend to grow more significantly at night, and our experimental findings support this observation (Zhu et al., 2021; Zweifel et al., 2021).

### 3.4. Monitoring sucrose uptake through stomata in Japanese cedar

After successfully testing our needle-type BFC sensor for sucrose sensing in strawberry guava, we proceeded to test the real-time monitoring of sucrose uptake through stomata –to the best of our knowledge, for the first time. We used Japanese cedar as our model species (Fig. 4a). In our experiments, we employed two types of water with stable differences in the isotopic composition of  $^{18}\text{O}$  and  $^{16}\text{O}$ : Alaskan water and Kitakyushu local water. This distinction allowed us to assess water transport through Japanese cedar leaves quantitatively, as explained in Section 2.6.

Japanese cedar used in the experiment was ordinarily grown in Kitakyushu water. Therefore, the amount of Alaskan water absorbed through the leaf surface could be determined by measuring the level of  $^{18}\text{O}$  (Fig. 4b). We varied light exposure by covering some leaves with aluminum foil (Fig. 4c) by immersing leaves in Alaskan water within plastic bags. After 8 h, we measured the  $^{18}\text{O}$  content in the plant using an isotope analyzer. As shown in Fig. 4d, the experimental group exposed to light had a higher  $^{18}\text{O}$  content than those kept in darkness, indicating that Japanese cedar leaves can absorb water through the leaf surface under light exposure, consistent with previous findings (Noda et al., 2025).

Moreover, to further investigate the movement of water molecules through the stomatal aperture, we devised a new protocol to identify plant-derived water molecules released into the exogenous bathing medium. This was achieved by detecting proton ( $^1\text{H}$ ) signals from  $\text{H}_2\text{O}$  molecules released into deuterium-based water ( $^2\text{H}_2\text{O}$ , or  $\text{D}_2\text{O}$ , purity 99.9 %). After immersing intact Sugi leaves into  $\text{D}_2\text{O}$ -filled plastic bags for up to 60 min, the migration of  $\text{H}_2\text{O}$  from the leaves was confirmed by monitoring the  $^1\text{H}$  signal in the  $\text{D}_2\text{O}$  medium using a benchtop  $^1\text{H}$ -NMR (NMReady60pro, Nanalysis Corp, Calgary, Canada).

The rate of water efflux was enhanced under light. When the kinetics of water movement was simulated with the Michaelis-Menten-like Hill-type equation ( $V = (V_{\max} t^n)/(K_t^n + t^n)$ , where  $V$  is the  $^1\text{H}$  signal intensity (arbitrary units),  $t$  is time (min),  $K_t$  is the apparent Michaelis constant, and  $n$  is the Hill coefficient) as a function of time,  $K_t$  recorded under the light was 1/3 of the one recorded in the dark (Fig. S4), suggesting that the time required for attaining the equilibrium was largely shortened under illumination. Specifically, the fitted curves revealed a lower  $K_t$  under backlight (BL;  $K_t = 14$ ) compared to dark ( $K_t = 41$ ), indicating faster water exchange under light-stimulated stomatal opening. Thus, our analysis supports the role of water translocation across the light-stimulated aperture of the stomata in Sugi leaves. Since sucrose is water-soluble, we also investigated whether sucrose could enter the plant body along with water absorbed through the leaves. To explore this, we used the sucrose sensor developed in this study to monitor real-time sucrose concentrations in Japanese cedar and inserted the needle into a branch (Fig. S5). Chronoamperometry was used at the potential of +0.6 V, to determine the current density reflecting the sucrose concentration (Fig. 4e). The experiment began after 4 h in order for the current to reach a plateau and to achieve a stable experimental environment. At the 4-h mark, the Japanese cedar leaves were immersed into a 50 mM sucrose solution, and light exposure was alternated every 4 h.

During the 4 to 8-h measurement period, the sucrose concentration

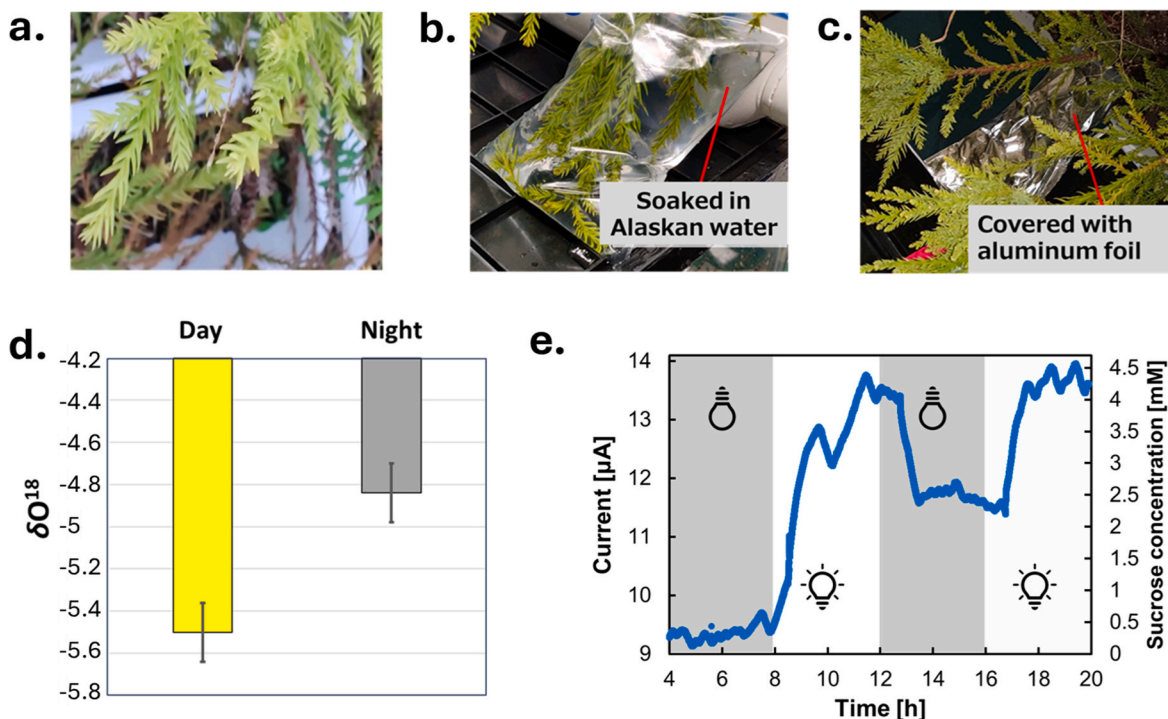


**Fig. 4. Real-time monitoring of changes in sucrose levels in Japanese cedar reflecting the light-dependent uptake of sucrose solution through stomata.** Evidence of the intake of foreign water differed in isotopic property through intact leaf surface of Sugi seedling: a) intact leaf of Sugi grown in local water with moderate  $\text{H}_2^{18}\text{O}$  content ( $\delta^{18}\text{O} = -5.05$ ); b) leaf tissue soaked in foreign water (Alaskan water with low  $\text{H}_2^{18}\text{O}$  content ( $\delta^{18}\text{O} = -16.53$ ); c) leaf soaked in Alaskan water but covered with aluminum foil as dark control; d) comparison of  $\delta^{18}\text{O}$  values in leaf water extracted after 8 h of incubation with Alaskan water under daylight or in the dark, average and standard deviation were calculated from  $n = 3$ . e): Real-time chronoamperometric ( $V = +0.6\text{V}$  vs BOD biocathode) monitoring of sucrose concentration in Japanese cedar soaked in 50 mM sucrose in different light conditions (4–8 h: light-off, 8–12 h: light-on, 12–16 h: light-off, 16–20 h: light-on).

detected under dark conditions showed only minor changes, similar to those observed in Fig. 3c(ii), presumably originating in the plant's intrinsic metabolic activity. This observation suggests that without light, the stomata remain closed, preventing water and sucrose entry into the plant, and only the plant's internal sugar transport was active. Between 8 and 12 h, with light exposure, the stomata opened, enabling water and sucrose absorption through the leaves, resulting in a marked increase in sucrose concentration. Despite some variability, a clear upward trend in sucrose concentration was observed.

At 12 h, the light was turned off, and as the absorbed sucrose was gradually transported to other parts of the plant, the sucrose concentration in the measured area decreased rapidly. However, the concentration remained higher than that during the 4 to 8-h period, presumably due to the initial high sucrose uptake. This may also be due to the plant's instability to transport and store large amounts of sucrose in a short time. At 16 h, the light was reintroduced, initiating the same water absorption process and causing a subsequent rise in sucrose concentration. Interestingly, the peak sucrose concentration during this period (4.5 mM) was comparable to that observed between 8 and 12 h (4.5 mM), suggesting a saturation limit for sucrose absorption through the leaves of the tested Japanese cedar. Taken together, we successfully demonstrated real-time monitoring of sucrose levels in Japanese cedar ('Sugi') introduced through stomatal uptake for the first time using a BFC-type multienzyme biosensor.

To further evaluate the reproducibility and operational stability of the device, we monitored the sensor's response over a three-day period by inserting it into a Sugi branch with young leaves immersed in 50 mM sucrose solution. The plant underwent light/dark cycles every 12 h, consistent with standard cultivation conditions. As shown in Fig. S6, the sensor exhibited a response pattern over the first two days that closely resembled the trend observed in Fig. 4e, confirming the reproducibility of the device under similar experimental conditions. On the third day, a moderate fluctuation and decline in signals were observed, which we attribute to partial drying of the agarose gel and possible loss of enzymatic activity over time.

However, as demonstrated in the device lifetime test performed in 25 mM sucrose solution Fig. S7, the sensor retained 86 % of its initial signal after 72 h of continuous measurement, suggesting that the overall operational stability remains acceptable for extended use.

It is observed that when the lighting condition changes, the signal changes with a lag of about 45 min, which is greater than the 90 s response time of the sensor. Therefore, the lag time is limited by the sucrose transport speed in the phloem of the plant. In plant physiology, phloem transport of sucrose occurs on the timescale of minutes to hours, depending on the plant species, environmental conditions, and source-sink activity. For instance, studies using radiolabeled carbon or fluorescent tracers have reported sucrose transport speeds ranging from 1 to 10 mm per minute in higher plants (Giaquinta, 1983; Turgeon, 2010). As sucrose accumulation or depletion due to processes such as stomatal regulation, photosynthetic activity, or circadian rhythms typically evolves over periods longer than a few minutes, the sensor's response time is acceptable for real-time physiological monitoring in intact plants.

These experimental results highlight the sensor's capability to monitor dynamic changes in sugar levels under varying environmental conditions. Such real-time monitoring opens new possibilities for connecting plant metabolic activity with practical agricultural management. Photosynthesis and translocation of sugars, chiefly in the forms of glucose and sucrose, determine the growth rate and eventually yield of starch and biomass in all agricultural crops. Therefore, monitoring the photosynthetic productivity and utilization of the photosynthetic products within the living plants is the key to predicting the agricultural productivity both in the field and under horticultural facilities such as greenhouses. In order to simulate and control plant growth based on mathematical models (Kawano et al., 2020; Okamoto et al., 2016), several researchers are engaged in the monitoring and simulation of

photosynthetic performance of individual plants under changing environmental conditions (Okamoto et al., 2016). However, successful systemic allocation through finely controlled translocation of the photosynthetic products among the plant organs meeting the changing local demands must be the missing piece among the key parameters to assess the orchestrated growth of whole plants. Therefore, the application of our novel plant-insertable sensors, allowing the real-time monitoring of the dynamic translocation of the sugars within the living plants, may provide novel tools for agricultural researchers and field agricultural engineers. In future work, applying this platform to other plant organs such as leaves, roots, and seeds, may offer valuable insights, for example, sink dynamics, root exudation processes, and sugar mobilization during seed germination, enabling a more complete understanding of whole-plant physiological coordination.

It should be noted that plant sap contains various secondary metabolites such as phenolic compounds, which may potentially interfere with enzymatic reactions. In this system, only GOD is directly involved in generating the electrochemical signal. Although some phenolic compounds have been reported to inhibit GOD activity in peroxidase-coupled colorimetric assays (Wong and Huang, 2014), our sensor uses direct electrochemical detection, which minimizes such interference. Furthermore, both enzymes are present in excess and do not participate in redox reactions. Therefore, we consider the impact of such interference to be negligible in our measurements. Nevertheless, a more systematic investigation of interference from plant-derived metabolites would be valuable in future studies.

The current needle-type biosensor was applied in a one-time measurement fashion under controlled laboratory conditions, and localized insertion into lignified tissues such as stems or branches was used to minimize physiological impact. Although some tissue disruption is inevitable, the effect remains limited to the insertion site and does not significantly influence overall plant function during short-term monitoring. In future practical applications, the electrode housing and insertion interface can be further optimized depending on the structural properties of different plant species. For instance, microneedle-based electrodes, thinner tips, or flexible substrates may reduce invasiveness and potentially allow repeated measurements. These engineering improvements would expand the sensor's applicability for long-term or field-based monitoring while minimizing plant stress.

#### 4. Conclusions

In this study, we developed a plant-insertable sucrose sensor featuring a multi-enzyme bioanode integrating glucose oxidase, invertase, and mutarotase, paired with a bilirubin oxidase-based biocathode. This sensor demonstrated rapid and reliable real-time monitoring of sucrose uptake through stomatal pathways, with a response time of 90 s for 0.1 mM sucrose and 2 min for 1.0 mM sucrose. The efficient electron transfer mediated by PVI-Os significantly enhanced the sensor's responsiveness and stability.

Experimental results indicated that the sensor could detect sucrose concentrations as low as 100  $\mu$ M, which was identified as the LOD, and a linear detection range of 100  $\mu$ M–60 mM, covering physiologically relevant sucrose concentrations in plants. Electrochemical measurements confirmed that the sensor remains functional across a temperature range from 10 °C to 40 °C, with enzymatic activity preserved and reversible changes observed in signal response, enabling its use under varying environmental conditions. Day-night monitoring of strawberry guava (*Psidium cattleianum*) revealed higher sucrose transport activity at night, consistent with the redistribution of photosynthetic sugars. Furthermore, experiments with isotopically labeled water demonstrated that Japanese cedar can absorb and transport both water and sucrose through stomatal pathways under light conditions.

These findings highlight the potential of this novel sucrose sensor for studying dynamic plant processes and its applicability in real-time monitoring of sugar transport across diverse plant species and

environmental conditions. Looking forward, future work should focus on enhancing the sensor's long-term durability and integrating wireless data transmission to facilitate remote monitoring in field settings. Additionally, expanding the sensor's application to a broader range of plant systems and agricultural environments could significantly contribute to precision agriculture and plant physiology research.

### CRedit authorship contribution statement

**Shiqi Wu:** Writing – review & editing, Writing – original draft, Visualization, Investigation, Formal analysis, Data curation, Conceptualization. **Wakutaka Nakagawa:** Investigation, Data curation. **Yuki Mori:** Investigation, Data curation. **Saman Azhari:** Writing – review & editing, Validation, Investigation. **Gábor Méhes:** Writing – review & editing, Validation. **Yuta Nishina:** Writing – review & editing, Resources. **Tomonori Kawano:** Writing – review & editing, Validation, Resources, Methodology, Investigation, Data curation. **Takeo Miyake:** Writing – review & editing, Visualization, Validation, Supervision, Resources, Project administration, Methodology, Funding acquisition, Conceptualization.

### Declaration of competing interest

The authors declare the following financial interests/personal relationships which may be considered as potential competing interests: Miyake Takeo reports financial support were provided by Japan Society for the Promotion of Science Agency, Japan and Japan Science and Technology Agency, Japan. If there are other authors, they declare that they have no known competing financial interests or personal relationships that could have appeared to influence the work reported in this paper.

### Acknowledgements

This study was supported by KAKENHI and PRESTO (Grant Number: JPMJPR20B8). A portion of this work was conducted at the Kitakyushu Foundation for the Advancement of Industry, Science, and Technology, Semiconductor Center, and supported by the Nanotechnology Platform Program of the Ministry of Education, Culture, Sports, Science, and Technology, Japan.

### Appendix A. Supplementary data

Supplementary data to this article can be found online at <https://doi.org/10.1016/j.bios.2025.117674>.

### Data availability

Data will be made available on request.

### References

- Alberto, F., Bignon, C., Sulzenbacher, G., Henrissat, B., Czjzek, M., 2004. The three-dimensional structure of invertase ( $\beta$ -Fructosidase) from *Thermotoga maritima* reveals a bimodular arrangement and an evolutionary relationship between retaining and inverting glycosidases. *J. Biol. Chem.* 279, 18903–18910. <https://doi.org/10.1074/jbc.M313911200>.
- Alvau, M.D., Tartaggia, S., Meneghello, A., Casetta, B., Calia, G., Serra, P.A., Polo, F., Toffoli, G., 2018. Enzyme-based electrochemical biosensor for therapeutic drug monitoring of anticancer drug irinotecan. *Anal. Chem.* 90, 6012–6019. <https://doi.org/10.1021/acs.analchem.7b04357>.
- Berry, Z.C., Emery, N.C., Gotsch, S.G., Goldsmith, G.R., 2019. Foliar water uptake: processes, pathways, and integration into plant water budgets. *Plant Cell Environ.* 42, 410–423. <https://doi.org/10.1111/pce.13439>.
- Bihar, E., Deng, Y., Miyake, T., Saadaoui, M., Malliaras, G.G., Rolandi, M., 2016. A disposable paper breathalyzer with an alcohol sensing organic electrochemical transistor. *Sci. Rep.* 6, 27582. <https://doi.org/10.1038/srep27582>.
- Boanares, D., Isaías, R.R.M.S., de Sousa, H.C., Kozovits, A.R., 2018. Strategies of leaf water uptake based on anatomical traits. *Plant Biol.* 20, 848–856. <https://doi.org/10.1111/plb.12832>.

- Bruen, D., Delaney, C., Florea, L., Diamond, D., 2017. Glucose sensing for diabetes monitoring: recent developments. *Sensors* (Peterb., NH) 17, 1866. <https://doi.org/10.3390/s17081866>.
- Cao, Y.-Y., Yang, M.-T., Chen, S.-Y., Zhou, Z.-Q., Li, X., Wang, X.-J., Bai, J.-G., 2015. Exogenous sucrose influences antioxidant enzyme activities and reduces lipid peroxidation in water-stressed cucumber leaves. *Biol. Plant. (Prague)* 59, 147–153. <https://doi.org/10.1007/s10535-014-0469-7>.
- Chen, H., Zhou, S., Chen, J., Zhou, J., Fan, K., Pan, Y., Ping, J., 2024. An integrated plant glucose monitoring system based on microneedle-enabled electrochemical sensor. *Biosens. Bioelectron.* 248, 115964. <https://doi.org/10.1016/j.bios.2023.115964>.
- Chiba, S., 1997. Molecular mechanism in  $\alpha$ -Glucosidase and glucoamylase. *Biosci. Biotechnol. Biochem.* 61, 1233–1239. <https://doi.org/10.1271/bbb.61.1233>.
- Chin, A.R.O., Guzmán-Delgado, P., Kerhoulas, L.P., Zwieniecki, M.A., 2023. Acclimation of interacting leaf surface traits affects foliar water uptake. *Tree Physiol.* 43, 418–429. <https://doi.org/10.1093/treephys/tpac120>.
- Dawson, T.E., Goldsmith, G.R., 2018. The value of wet leaves. *New Phytol.* 219, 1156–1169. <https://doi.org/10.1111/nph.15307>.
- Diacci, C., Abedi, T., Lee, J.W., Gabriellson, E.O., Berggren, M., Simon, D.T., Niittylä, T., Stavrinidou, E., 2021. Diurnal *in vivo* xylem sap glucose and sucrose monitoring using implantable organic electrochemical transistor sensors. *iScience* 24, 101966. <https://doi.org/10.1016/j.isci.2020.101966>.
- Gavrilaş, S., Ursachi, C., Ştefan, Perța-Crişan, S., Munteanu, F.-D., 2022. Recent trends in biosensors for environmental quality monitoring. *Sensors* (Peterb., NH) 22, 1513. <https://doi.org/10.3390/s22041513>.
- Giaquinta, R.T., 1983. Phloem loading of sucrose. *Annu. Rev. Plant Biol.* 34, 347–387. <https://doi.org/10.1146/annurev.pp.34.060183.002023>.
- Guzmán-Delgado, P., Laca, E., Zwieniecki, M.A., 2021. Unravelling foliar water uptake pathways: the contribution of stomata and the cuticle. *Plant Cell Environ.* 44, 1728–1740. <https://doi.org/10.1111/pce.14041>.
- Hamid, J.A., Moody, G.J., Thomas, J.D.R., 1988. Chemically immobilised tri-enzyme electrode for the determination of sucrose using flow injection analysis. *Analyst* 113, 81–85. <https://doi.org/10.1039/AN9881300081>.
- Hemdan, M., Ali, M.A., Doghish, A.S., Mageed, S.S.A., Elazab, I.M., Khalil, M.M., Mabrouk, M., Das, D.B., Amin, A.S., 2024. Innovations in biosensor technologies for healthcare diagnostics and therapeutic drug monitoring: applications, recent progress, and future research challenges. *Sensors* (Peterb., NH) 24, 5143. <https://doi.org/10.3390/s24165143>.
- Huang, Y., Xu, J., Liu, J., Wang, X., Chen, B., 2017. Disease-related detection with electrochemical biosensors: a review. *Sensors* (Peterb., NH) 17, 2375. <https://doi.org/10.3390/s17102375>.
- Huber, S.C., Huber, J.L., 1992. Role of sucrose-phosphate synthase in sucrose metabolism in leaves 1. *Plant Physiol* 99, 1275–1278. <https://doi.org/10.1104/pp.99.4.1275>.
- Hudson, C.S., 1910. A review of discoveries on the mutarotation of the SUGARS.2. *J. Am. Chem. Soc.* 32, 889–894. <https://doi.org/10.1021/ja01925a009>.
- Ispas, C.R., Crivat, G., Andreescu, S., 2012. Review: recent developments in enzyme-based biosensors for biomedical analysis. *Anal. Lett.* 45, 168–186. <https://doi.org/10.1080/00032719.2011.633188>.
- Justino, C.L.L., Duarte, A.C., Rocha-Santos, T.A.P., 2017. Recent progress in biosensors for environmental monitoring: a review. *Sensors* (Peterb., NH) 17, 2918. <https://doi.org/10.3390/s17122918>.
- Kai, H., Yamauchi, T., Ogawa, Y., Tsubota, A., Magome, T., Miyake, T., Yamasaki, K., Nishizawa, M., 2017. Accelerated wound healing on skin by electrical stimulation with a bioelectric plaster. *Adv. Healthcare Mater.* 6, 1700465. <https://doi.org/10.1002/adhm.201700465>.
- Kawano, T., Wallbridge, N., Plummer, C., 2020. Logistic models for simulating the growth of plants by defining the maximum plant size as the limit of information flow. *Plant Signal. Behav.* 15. <https://doi.org/10.1080/15592324.2019.1709718>.
- Knoche, M., 2015. Water uptake through the surface of fleshy soft fruit: barriers, mechanism, factors, and potential role in cracking. In: Kanayama, Y., Kochetov, A. (Eds.), *Abiotic Stress Biology in Horticultural Plants*. Springer, Japan, Tokyo, pp. 147–166. [https://doi.org/10.1007/978-4-431-55251-2\\_11](https://doi.org/10.1007/978-4-431-55251-2_11).
- Kulkarni, M.B., Ayachit, N.H., Aminabhavi, T.M., 2022. Biosensors and microfluidic biosensors: from fabrication to application. *Biosensors* 12, 543. <https://doi.org/10.3390/bios12070543>.
- Lastdrager, J., Hanson, J., Smeekens, S., 2014. Sugar signals and the control of plant growth and development. *J. Exp. Bot.* 65, 799–807. <https://doi.org/10.1093/jxb/ert474>.
- Lemoine, R., La Camera, S., Atanassova, R., Dédaldéchamp, F., Allario, T., Pourtau, N., Bonnemain, J.-L., Laloi, M., Coutos-Thévenot, P., Mauroussel, L., Faucher, M., Girousse, C., Lemonnier, P., Parrilla, J., Durand, M., 2013. Source-to-sink transport of sugar and regulation by environmental factors. *Front. Plant Sci.* 4. <https://doi.org/10.3389/fpls.2013.00272>.
- Li, S., Li, H., Lu, Y., Zhou, M., Jiang, S., Du, X., Guo, C., 2023. Advanced textile-based wearable biosensors for healthcare monitoring. *Biosensors* 13, 909. <https://doi.org/10.3390/bios13100909>.
- Louise Hovland\*, K., Sekse, L., 2004. Water uptake through sweet cherry (*Prunus avium* L.) fruit pedicels: influence of fruit surface water status and intact fruit skin. *Acta Agric. Scand., Sect. B* 54, 91–96. <https://doi.org/10.1080/09064710410024444>.
- Lu, T., Ji, S., Jin, W., Yang, Q., Luo, Q., Ren, T., 2023. Biocompatible and long-term monitoring strategies of wearable, ingestible and implantable biosensors: reform the next generation healthcare. *Sensors* (Peterb., NH) 23.
- Makaram, P., Owens, D., Aceros, J., 2014. Trends in nanomaterial-based non-invasive diabetes sensing technologies. *Diagnostics* 4, 27–46. <https://doi.org/10.3390/diagnostics4020027>.

- Mano, N., 2019. Engineering glucose oxidase for bioelectrochemical applications. *Bioelectrochemistry* 128, 218–240. <https://doi.org/10.1016/j.bioelechem.2019.04.015>.
- Miyake, T., Haneda, K., Nagai, N., Yatagawa, Y., Onami, H., Yoshino, S., Abe, T., Nishizawa, M., 2011a. Enzymatic biofuel cells designed for direct power generation from biofluids in living organisms. *Energy Environ. Sci.* 4, 5008–5012. <https://doi.org/10.1039/C1EE02200H>.
- Miyake, T., Yoshino, S., Yamada, T., Hata, K., Nishizawa, M., 2011b. Self-regulating enzyme–nanotube ensemble films and their application as flexible electrodes for biofuel cells. *J. Am. Chem. Soc.* 133, 5129–5134. <https://doi.org/10.1021/ja111517e>.
- Noda, K., Nakamura, A., Hamatake, K., Tanaka, T., Ikeda, R., Kawano, T., 2025. Enhanced liquid water intake by growing lettuce leaves via blue light-stimulated stomatal opening. *Hortic. Sci.* 38. <https://doi.org/10.36253/ahsc-15494>.
- Ogawa, Y., Kato, K., Miyake, T., Nagamine, K., Ofuji, T., Yoshino, S., Nishizawa, M., 2015. Organic transdermal iontophoresis patch with Built-in biofuel cell. *Adv. Healthcare Mater.* 4, 506–510. <https://doi.org/10.1002/adhm.201400457>.
- Okamoto, Y., Haraguchi, A., Suzuki, T., Kawano, T., 2016. New discussion on boysen-jensen's photosynthetic response curves under plant canopy and proposal of practical equations for monitoring and management of canopy photosynthesis. *Environ. Control Biol.* 54, 7–16. <https://doi.org/10.2525/ecb.54.7>.
- Pan, Z., Pitt, W.G., Zhang, Y., Wu, N., Tao, Y., Truscott, T.T., 2016. The upside-down water collection system of *Syntrichia caninervis*. *Nat. Plants* 2, 16076. <https://doi.org/10.1038/nplants.2016.76>.
- Perdomo, S.A., De la Paz, E., Del Caño, R., Seker, S., Saha, T., Wang, J., Jaramillo-Botero, A., 2023. Non-invasive in-vivo glucose-based stress monitoring in plants. *Biosens. Bioelectron.* 231, 115300. <https://doi.org/10.1016/j.bios.2023.115300>.
- Purcareia, C., Ruginescu, R., Banciu, R.M., Vasilescu, A., 2024. Extremozyme-based biosensors for environmental pollution monitoring: recent developments. *Biosensors* 14, 143. <https://doi.org/10.3390/bios14030143>.
- Ruan, Y.L., 2014. Sucrose metabolism: gateway to diverse carbon use and sugar signaling. *Annu. Rev. Plant Biol.* 65, 33–67. <https://doi.org/10.1146/annurev-arplant-050213-040251>.
- Scheller, F., Renneberg, R., 1983. Glucose-eliminating enzyme electrode for direct sucrose determination in glucose-containing samples. *Anal. Chim. Acta* 152, 265–269. [https://doi.org/10.1016/S0003-2670\(00\)84916-8](https://doi.org/10.1016/S0003-2670(00)84916-8).
- Secchi, F., Zwierniecki, M.A., 2016. Accumulation of sugars in the xylem apoplast observed under water stress conditions is controlled by xylem pH. *Plant. Cell Environ* 39, 2350–2360. <https://doi.org/10.1111/pce.12767>.
- Shankaran, D.R., Gobi, K.V., Miura, N., 2007. Recent advancements in surface plasmon resonance immunosensors for detection of small molecules of biomedical, food and environmental interest. *Sens. Actuators, B, Special Issue: 25th Anniversary of Sensors and Actuators B: Chemical* 121, 158–177. <https://doi.org/10.1016/j.snb.2006.09.014>.
- Song, Z., Zhou, S., Qin, Y., Xia, X., Sun, Y., Han, G., Shu, T., Hu, L., Zhang, Q., 2023. Flexible and wearable biosensors for monitoring health conditions. *Biosensors* 13, 630. <https://doi.org/10.3390/bios13060630>.
- Sturm, A., 1999. Invertases. Primary structures, functions, and roles in plant development and sucrose partitioning. *Plant Physiol.* 121, 1–8. <https://doi.org/10.1104/pp.121.1.1>.
- Tang, D., Ren, J., 2008. In situ amplified electrochemical immunoassay for carcinoembryonic antigen using horseradish peroxidase-encapsulated nanogold hollow microspheres as labels. *Anal. Chem.* 80, 8064–8870. <https://doi.org/10.1021/ac801091j>.
- Taniguchi, H., Akiyama, K., Fujie, T., 2020. Biopotential measurement of plant leaves with ultra-light and flexible conductive polymer nanosheets. *Bull. Chem. Soc. Jpn.* 93, 1007–1013. <https://doi.org/10.1246/bcsj.20200064>.
- Thoden, J.B., Holden, H.M., 2002. High resolution X-ray structure of galactose mutarotase from *Lactococcus lactis*. *J. Biol. Chem.* 277, 20854–20861. <https://doi.org/10.1074/jbc.M201415200>.
- Trommelen, J., Fuchs, C.J., Beelen, M., Lenaerts, K., Jeukendrup, A.E., Cermak, N.M., Van Loon, L.J.C., 2017. Fructose and sucrose intake increase exogenous carbohydrate oxidation during exercise. *Nutrients* 9, 167. <https://doi.org/10.3390/nu9020167>.
- Turgeon, R., 2010. The role of phloem loading Reconsidered12[W]. *Plant Physiol* 152, 1817–1823. <https://doi.org/10.1104/pp.110.153023>.
- Wang, L., Zhu, W., Zhang, J., Zhu, J.-J., 2023. Miniaturized microfluidic electrochemical biosensors powered by enzymatic biofuel cell. *Biosensors* 13, 175. <https://doi.org/10.3390/bios13020175>.
- Weng, G., Radojewski, P., Slotboom, J., 2023.  $\alpha$ -D-Glucose as a non-radioactive MRS tracer for metabolic studies of the brain. *Sci. Rep.* 13, 6159. <https://doi.org/10.1038/s41598-023-33161-8>.
- Wohlfahrt, G., Witt, S., Hendle, J., Schomburg, D., Kalisz, H.M., Hecht, H.-J., 1999. 1.8 and 1.9 Å resolution structures of the -Penicillium amagasakiense and Aspergillus niger glucose oxidases as a basis for modelling substrate complexes. *Acta Cryst. D* 55, 969–977. <https://doi.org/10.1107/S0907444999003431>.
- Wong, A.I.C., Huang, D., 2014. Assessment of the Degree of Interference of Polyphenolic Compounds on Glucose oxidation/peroxidase Assay. ACS Publications. <https://doi.org/10.1021/jf500431z> [WWW Document].
- Yan, F., Wang, F., Chen, Z., 2011. Aptamer-based electrochemical biosensor for label-free voltammetric detection of thrombin and adenosine. *Sens. Actuators, B* 160, 1380–1385. <https://doi.org/10.1016/j.snb.2011.09.081>.
- Ye, S., Feng, S., Huang, L., Bian, S., 2020. Recent progress in wearable biosensors: from healthcare monitoring to sports analytics. *Biosensors* 10, 205. <https://doi.org/10.3390/bios10120205>.
- Yin, S., Jin, Z., Miyake, T., 2019. Wearable high-powered biofuel cells using enzyme/carbon nanotube composite fibers on textile cloth. *Biosens. Bioelectron.* 141, 111471. <https://doi.org/10.1016/j.bios.2019.111471>.
- Yin, S., Liu, X., Kaji, T., Nishina, Y., Miyake, T., 2021. Fiber-crafted biofuel cell bracelet for wearable electronics. *Biosens. Bioelectron.* 179, 113107. <https://doi.org/10.1016/j.bios.2021.113107>.
- Yin, S., Liu, X., Kobayashi, Y., Nishina, Y., Nakagawa, R., Yanai, R., Kimura, K., Miyake, T., 2020. A needle-type biofuel cell using enzyme/mediator/carbon nanotube composite fibers for wearable electronics. *Biosens. Bioelectron.* 165, 112287. <https://doi.org/10.1016/j.bios.2020.112287>.
- Zhou, J., Liu, C., Yu, H., Tang, N., Lei, C., 2023. Research progresses and application of biofuel cells based on immobilized enzymes. *Appl. Sci.* 13, 5917. <https://doi.org/10.3390/app13105917>.
- Zhu, T., Fonseca De Lima, C.F., De Smet, I., 2021. The heat is on: how crop growth, development, and yield respond to high temperature. *J. Exp. Bot.* 72, 7359–7373. <https://doi.org/10.1093/jxb/erab308>.
- Zweifel, R., Sterck, F., Braun, S., Buchmann, N., Eugster, W., Gessler, A., Häni, M., Peters, R.L., Walthert, L., Wilhelm, M., Ziemnińska, K., Etzold, S., 2021. Why trees grow at night. *New Phytol.* 231, 2174–2185. <https://doi.org/10.1111/nph.17552>.